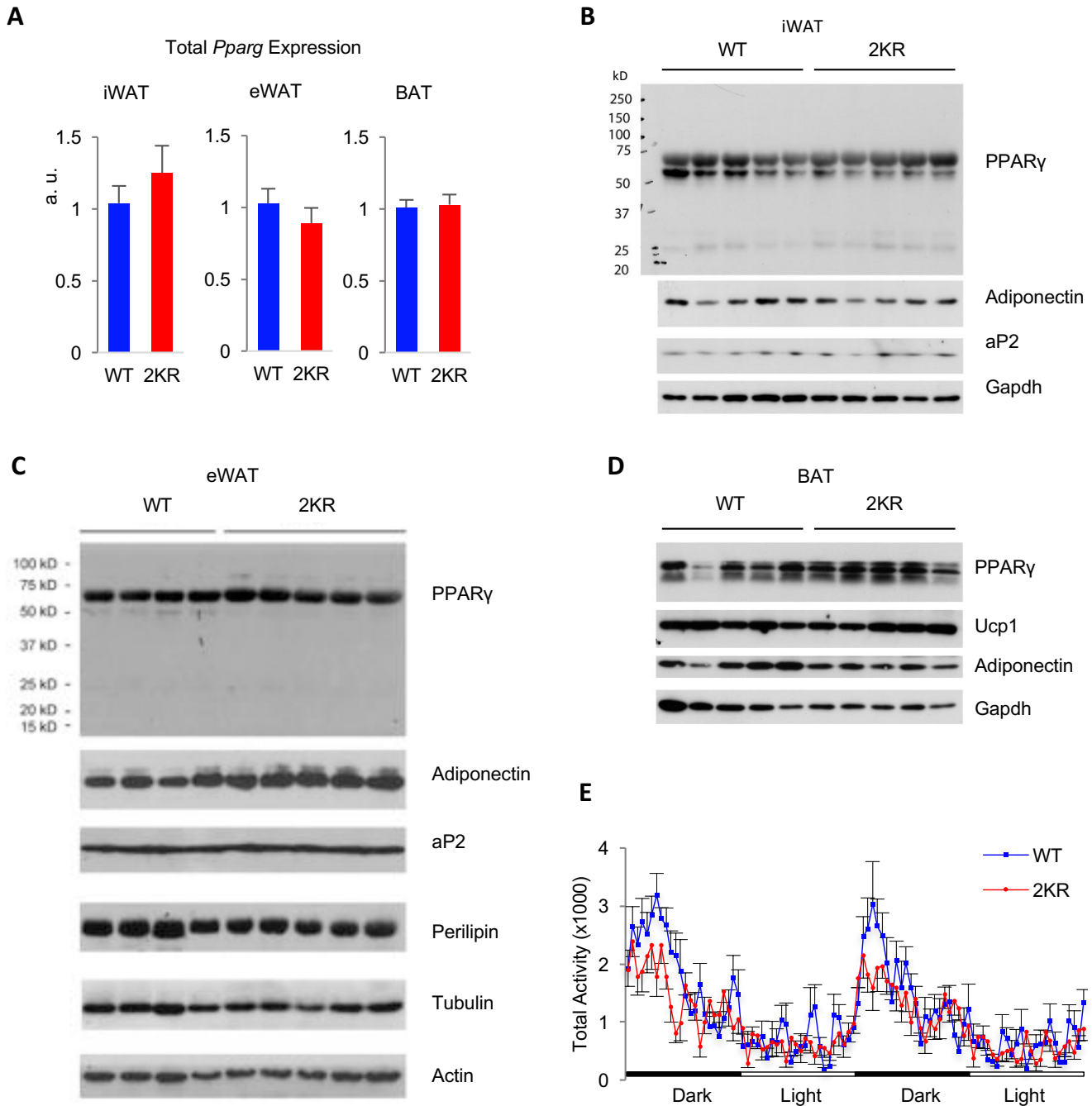
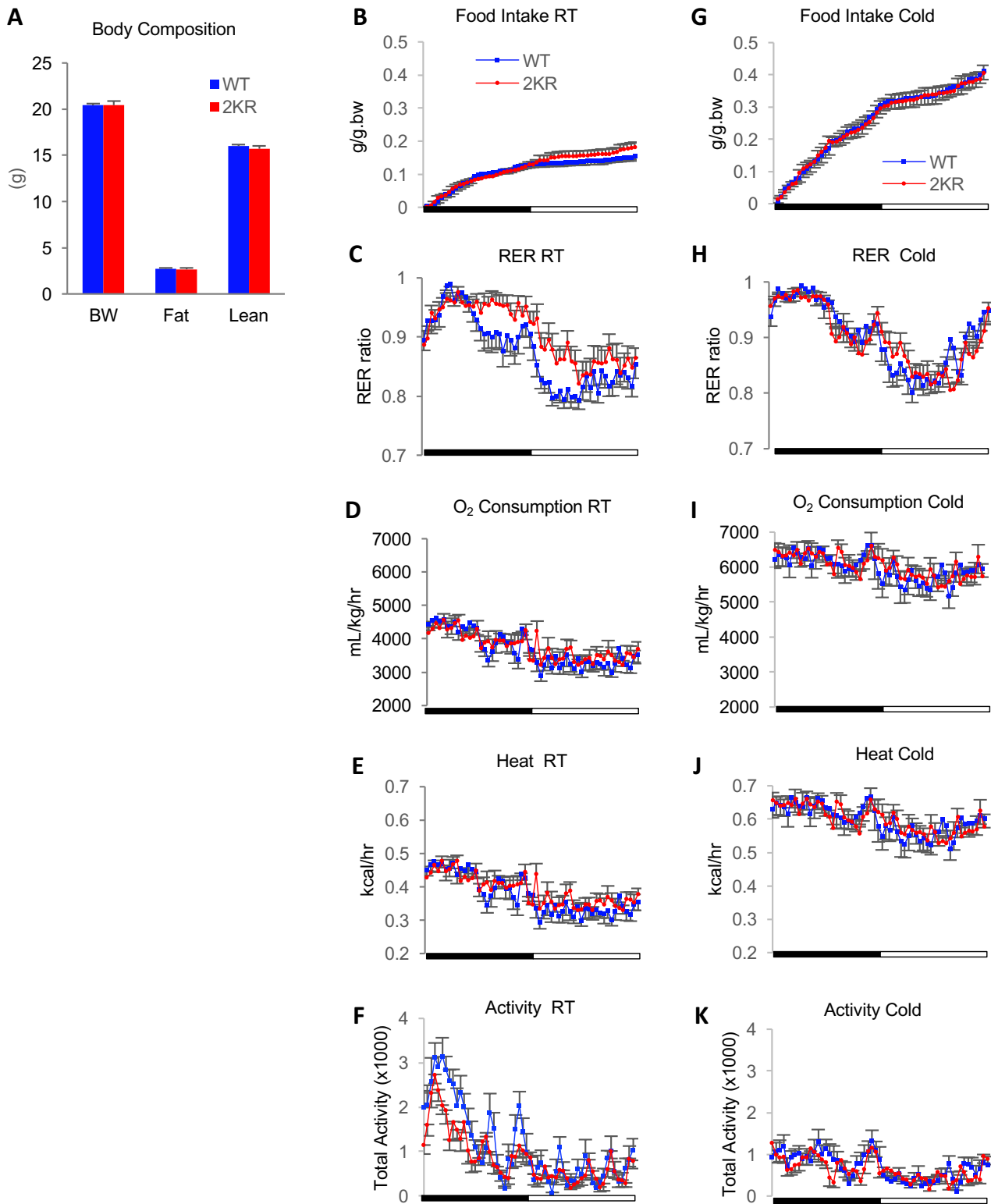


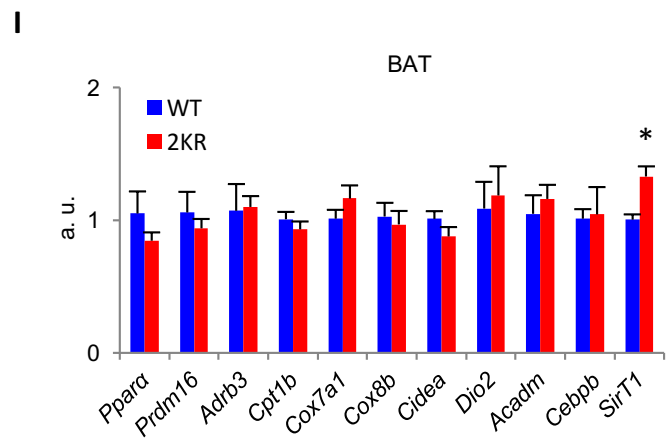
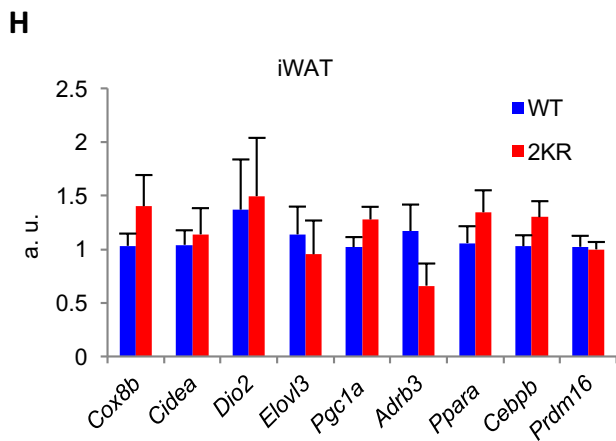
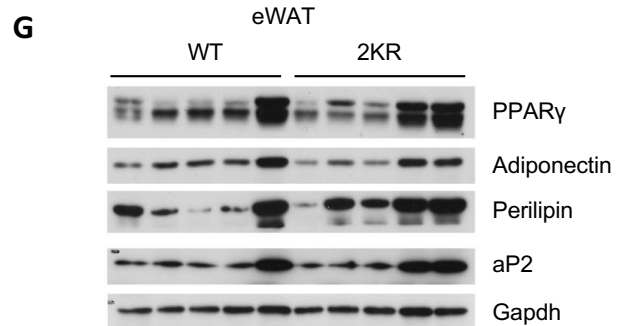
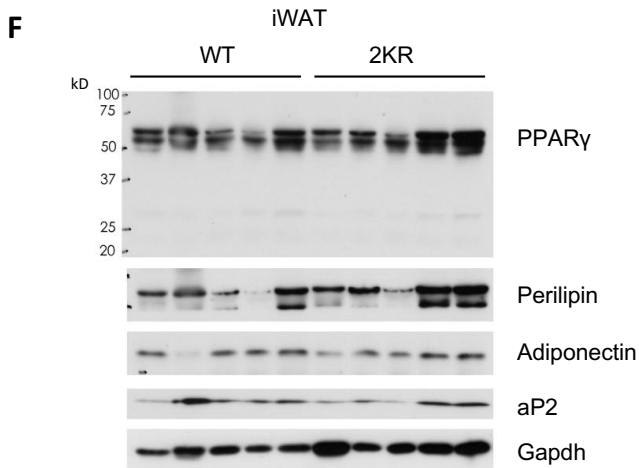
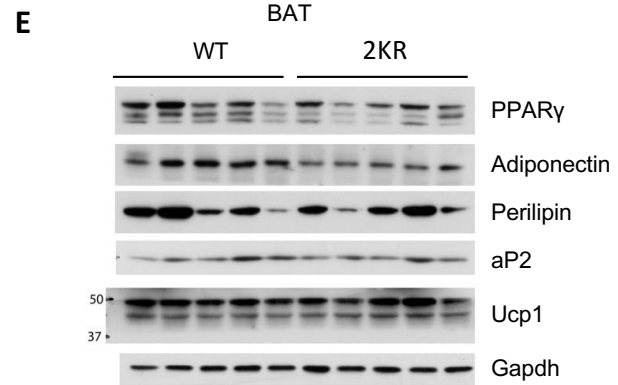
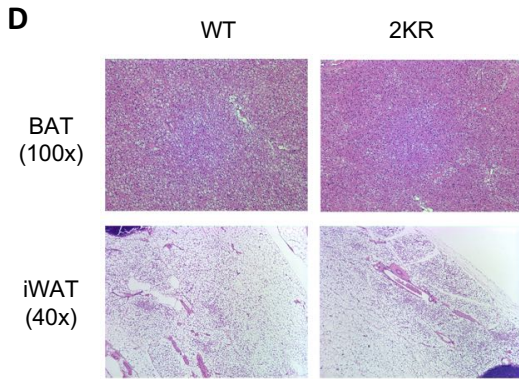
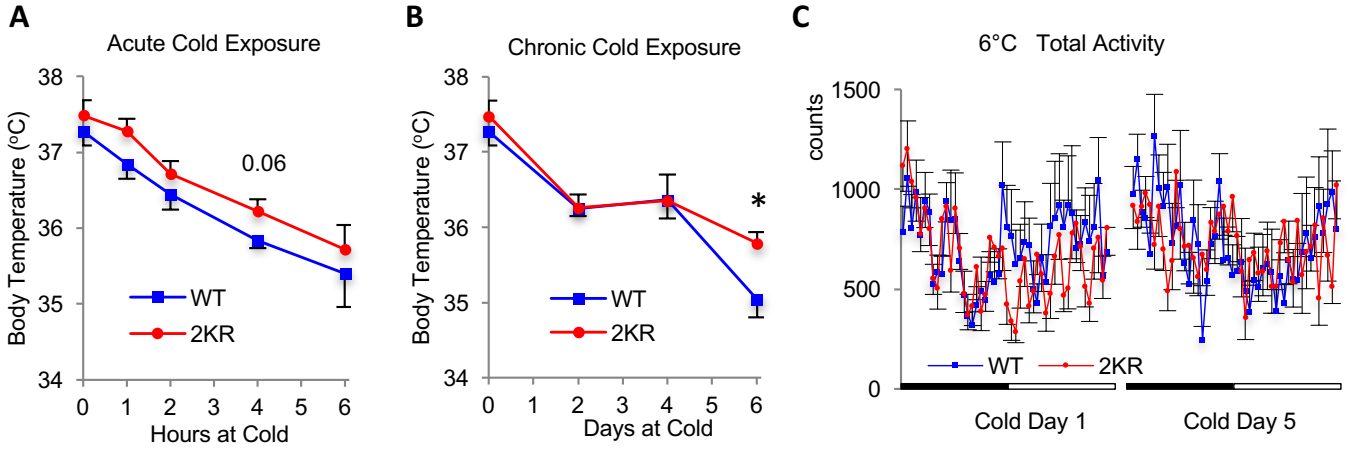
Supplemental Figure 1. Generation of deacetylation-mimetic 2KR knock-in mouse model. (A) Targeting scheme for generation of whole body 2KR knock-in mice. **(B)** PCR genotyping of WT, heterozygous (2KR/+) and homozygous (2KR/2KR) mice. The upper band is for WT allele and the lower band is for mutant 2KR allele. **(C)** Exon PCR in fat cDNA didn't detect altered PPAR γ isoforms. Primer design is illustrated in A.



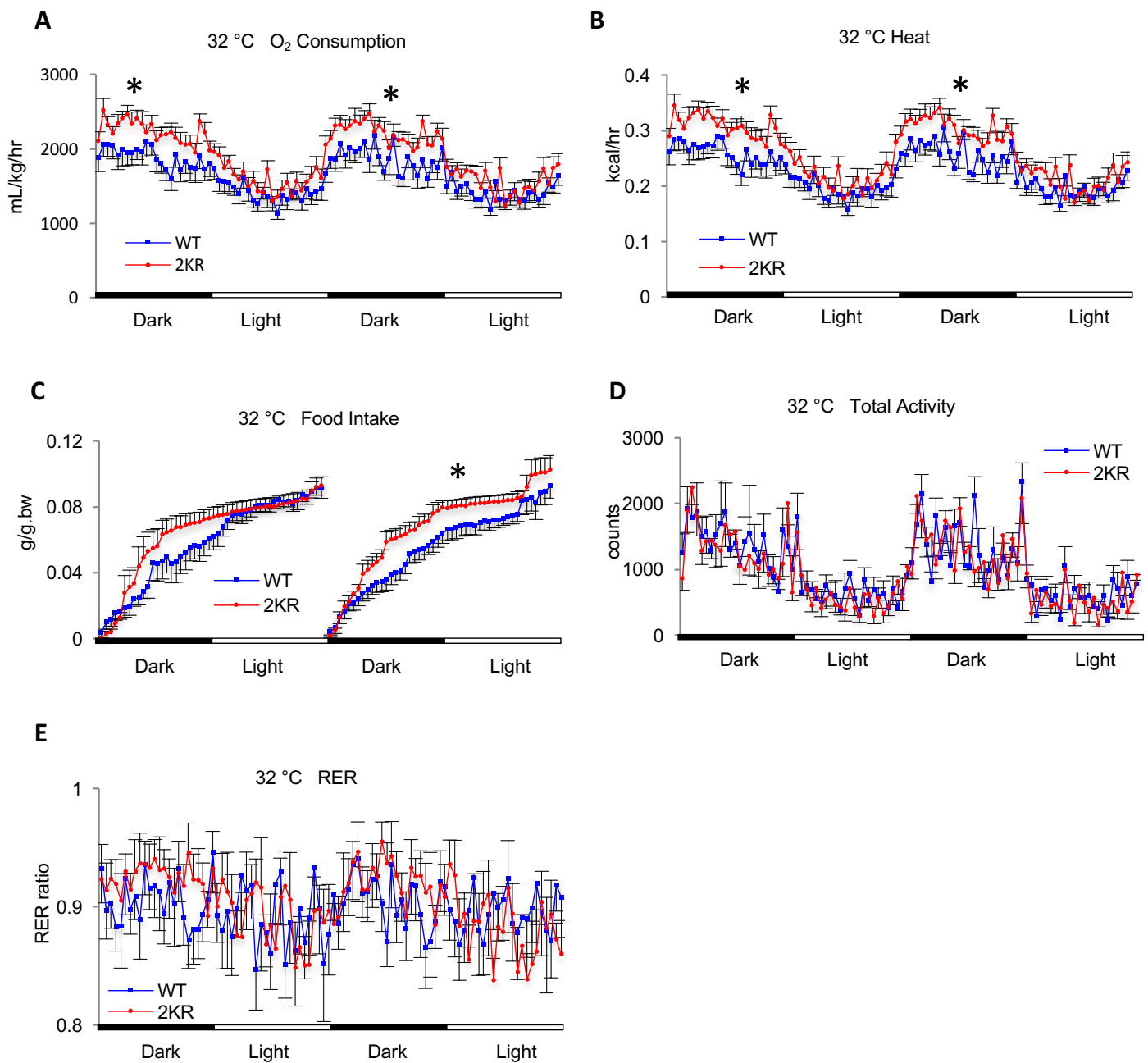
Supplemental Figure 2. Normal expression of adipose PPAR γ in deacetylation-mimetic 2KR mice. (A) Comparable expression of *Pparg* detected by qPCR in adipose tissues between WT and 2KR mice. **(B-D)** Western blotting analyses of iWAT (**B**), eWAT (**C**) and BAT (**D**) in 3-month old chow-fed mice. **(E)** Total activity in two constitutive days during calorimetric studies in chow-fed male mice (n=11, 12). Data represent means \pm SEM. Student's *t*-test was used for statistical analyses.



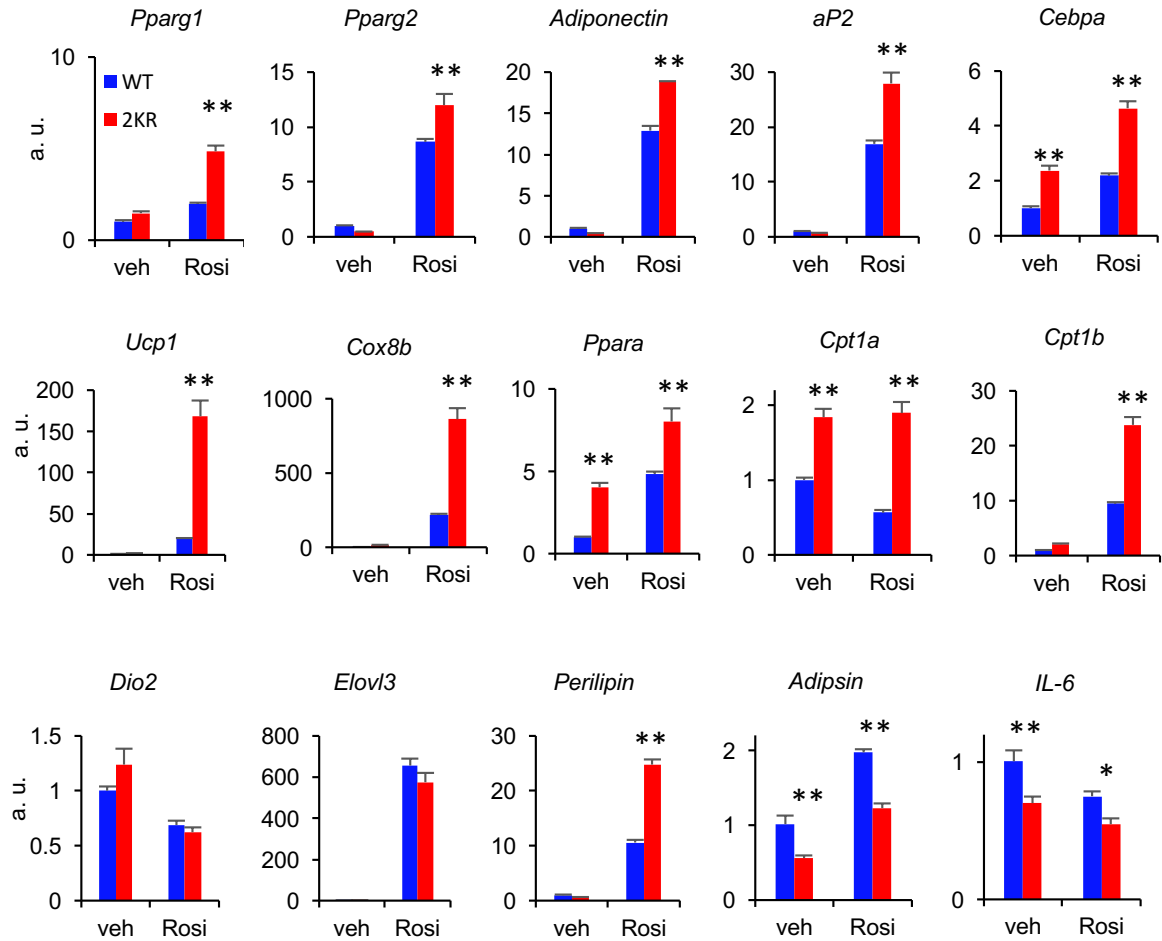
Supplemental Figure 3. Indirect calorimetric analyses of female mice. In 3-mon-old chow-fed female mice, body weight and composition (**A**), calorimetric analyses at room temperature (RT) (**B-F**) or cold exposure (cold) (**G-K**) (n=10, 10). Data represent means \pm SEM. Student's *t*-test was used for statistical analyses.



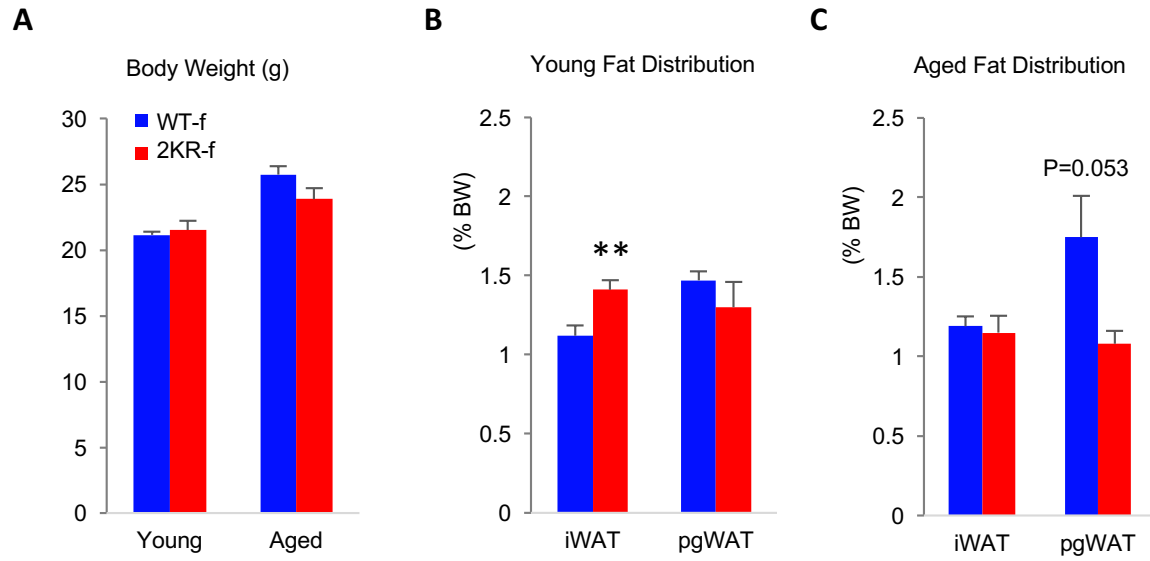
Supplemental Figure 4. Thermogenic response in 2KR male mice in the cold. (A-B) Body temperature change in chow-fed male mice at 8-month-old during acute (**A**) and chronic (**B**) cold challenge, * $p < 0.05$ (n=11, 11). (**C**) Total activities of 4-month-old male mice fed a chow diet during cold exposure (n=9, 11). (**D**) Representative Haematoxylin and Eosin (H&E) staining of adipose tissues from male mice after chronic cold exposure. Magnifications are at 100x (BAT) and 40x (iWAT). (**E-G**) Western blot analyses of adipose tissues from chronic cold challenged mice. (**H-I**) qPCR analyses of gene expression in inguinal WAT (iWAT) (**H**) and BAT (**I**) of chow-fed male mice at 5-6 month old after 5-day cold exposure, * $p < 0.05$ for WT vs. 2KR, n=6, 6. Data represent means \pm SEM. Student's *t*-test was used for statistical analyses.



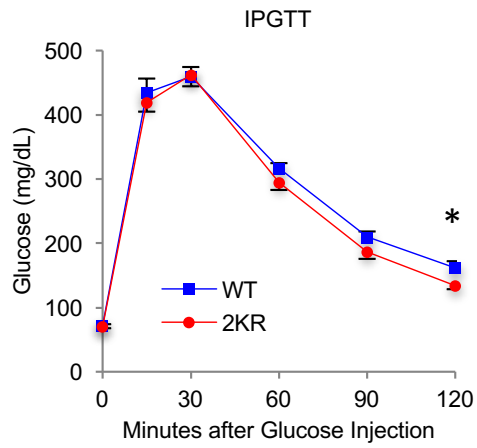
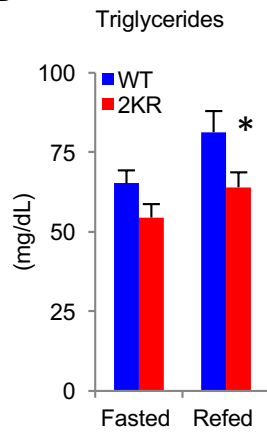
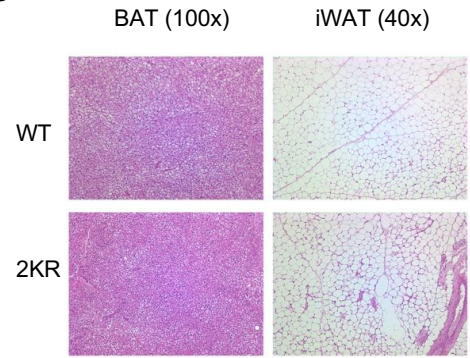
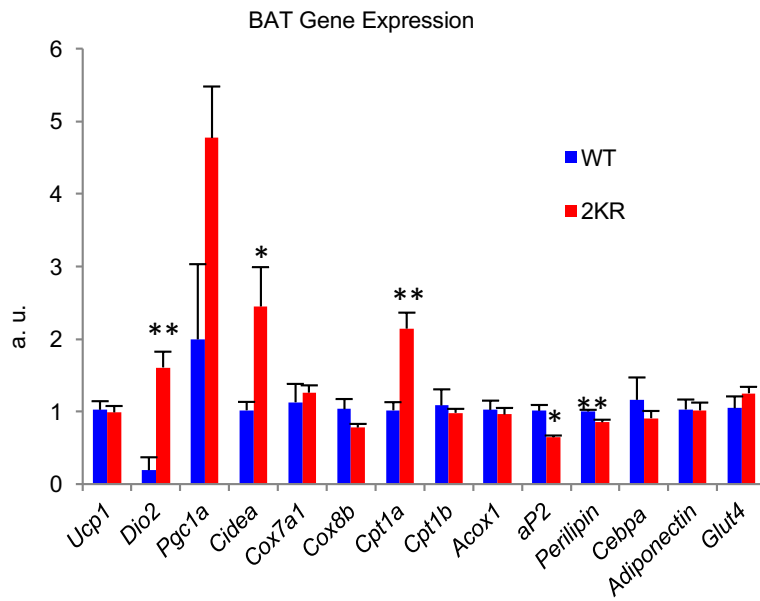
Supplemental Figure 5. Indirect calorimetric analyses of male 2KR mice at thermoneutrality. (A-E) Calorimetric analyses of 4-month-old male mice fed a chow diet at 32 °C. (A) Oxygen consumption; (B) Heat production; (C) Food intake; (D) Total activity and (E) Respiration exchange ratio (RER). *: $p < 0.05$ at multiple detection points, $n = 12$, 12. Data represent means \pm SEM. Student's t -test was used for statistical analyses.



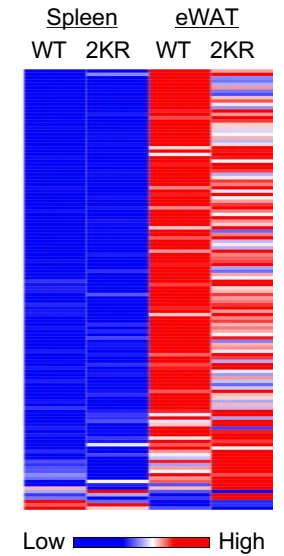
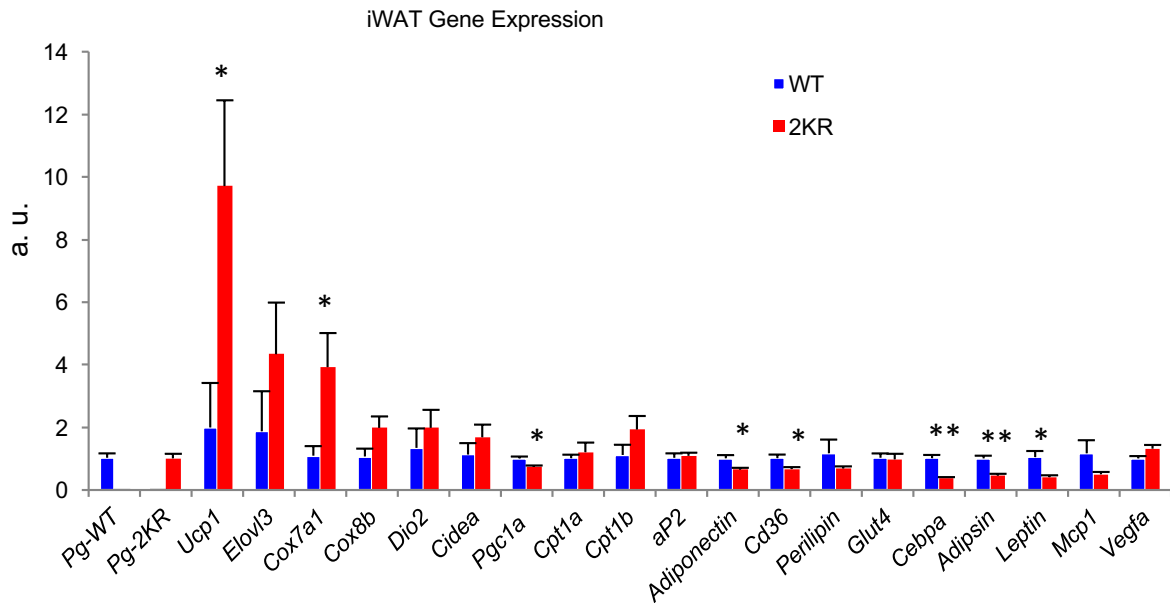
Supplemental Figure 6. The autonomous regulation of 2KR in primary adipocytes. qPCR analyses of gene expression in iWAT primary adipocytes differentiated without (veh) or with rosiglitazone (Rosi), * $p < 0.05$, ** $p < 0.01$ for WT vs. 2KR, $n = 3, 3$ (veh) and $4, 4$ (Rosi). Data represent means \pm SEM. Student's *t*-test was used for statistical analyses.



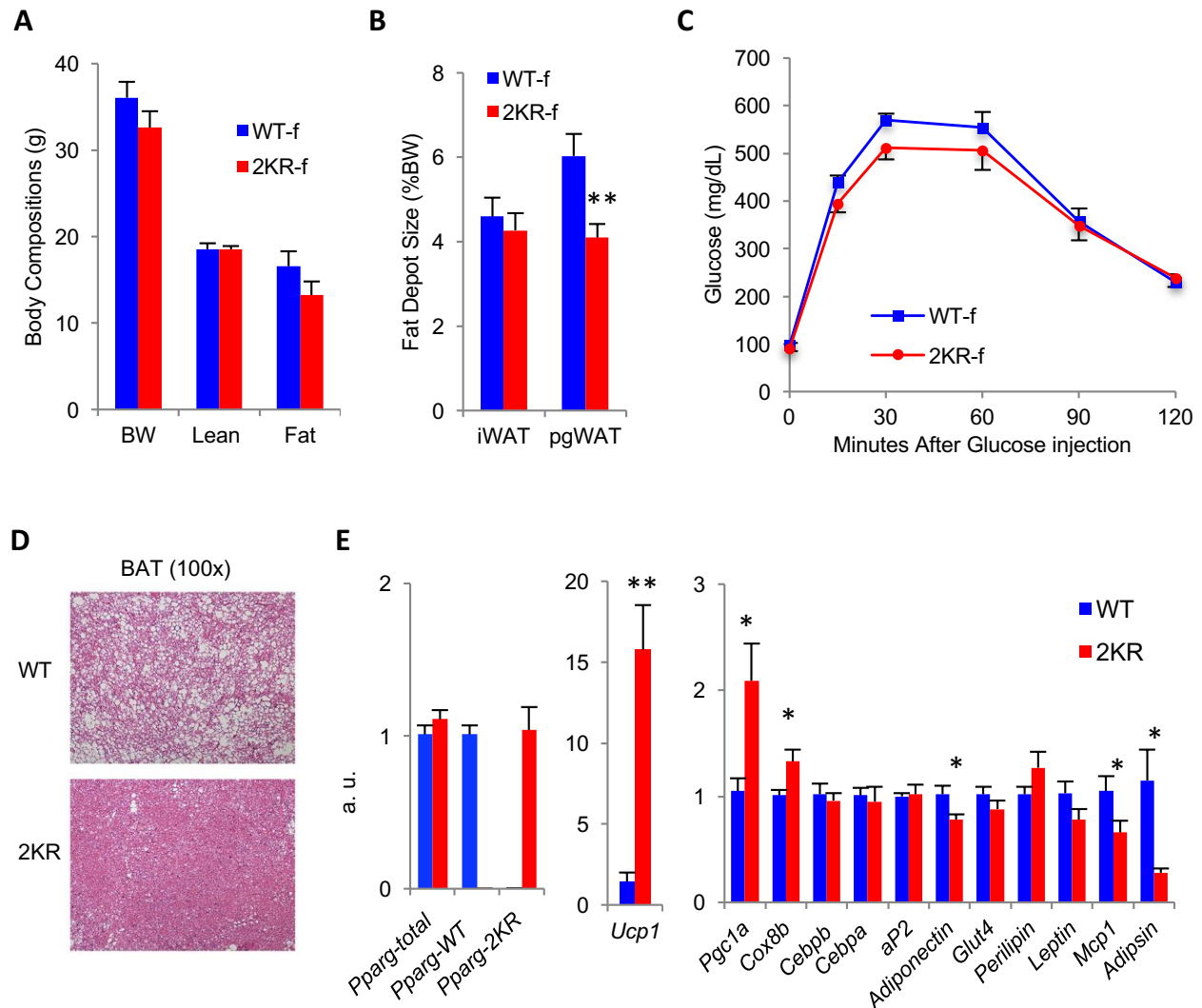
Supplemental Figure 7. Depot-specific effects of 2KR in female mice. In female mice, **(A)** body weight of young (3-mon-old) and aged (8-12-mon-old) mice; **(B)** increase of subcutaneous fat in young mice; **(C)** inhibition of visceral fat in aged mice. ** $p < 0.01$, $n = 8, 5, 5, 6$. Data represent means \pm SEM. Student's *t*-test was used for statistical analyses.

A**B****C****D****F**

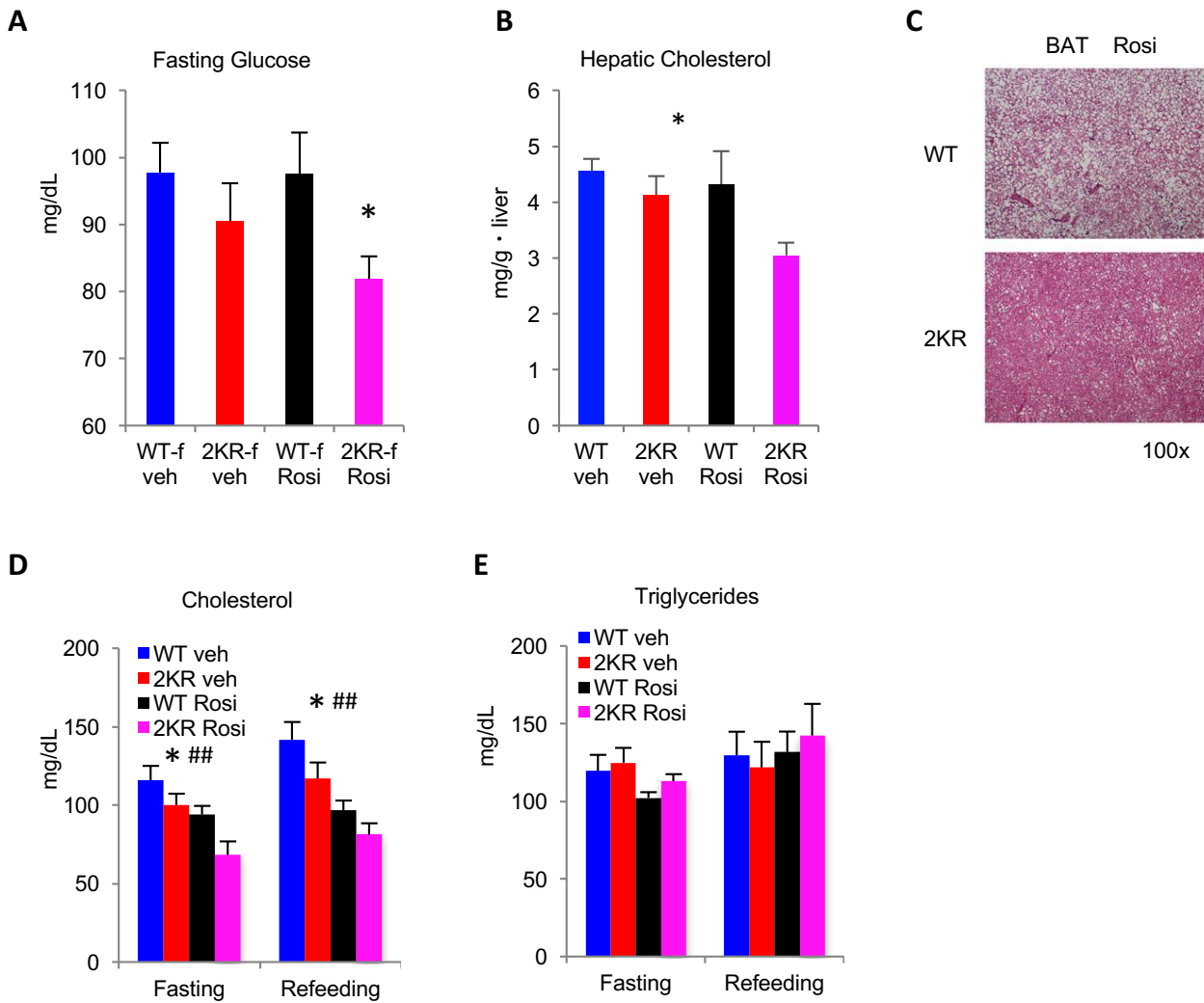
Fat Treg signature genes affected by S273A

**E**

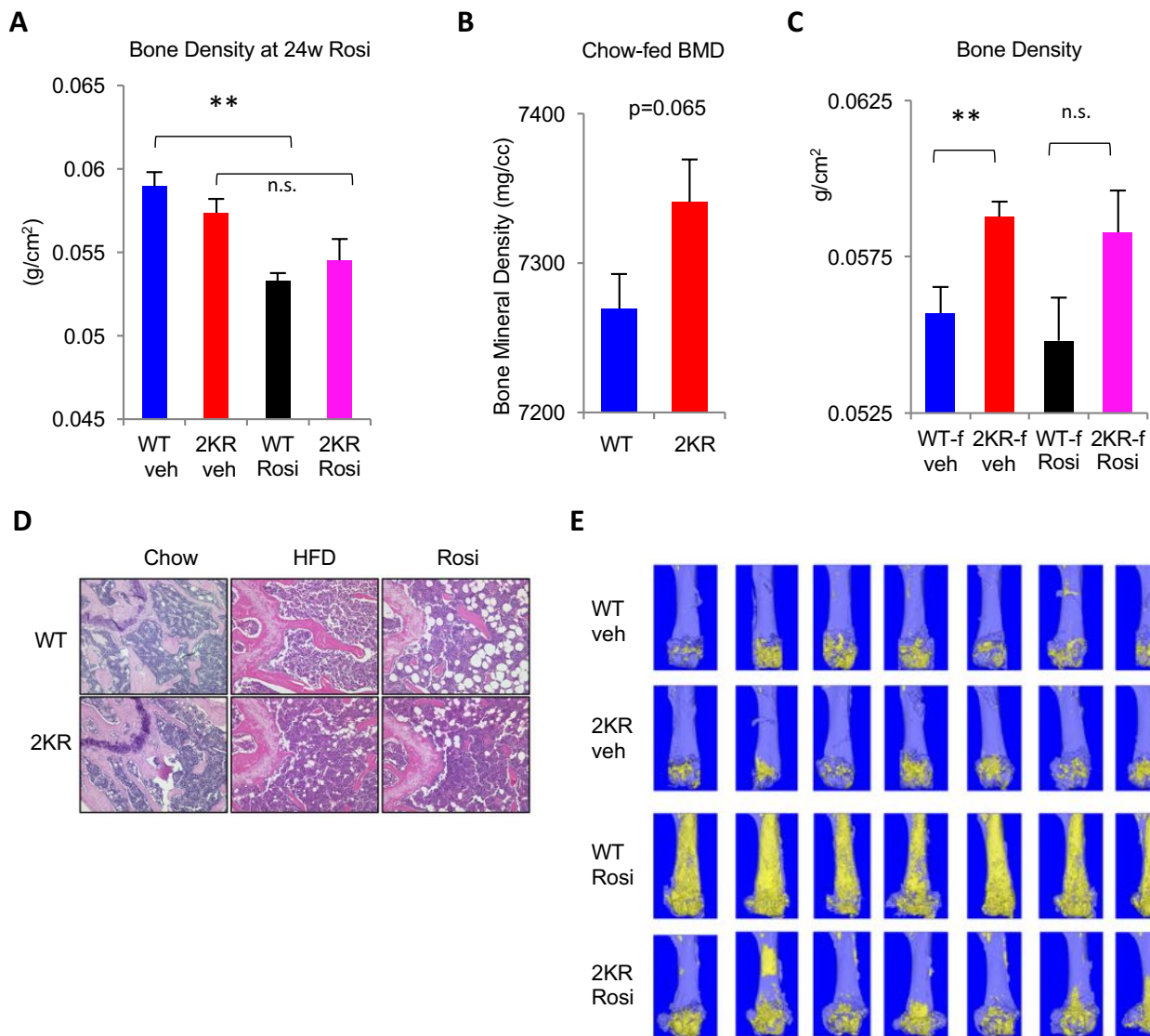
Supplemental Figure 8. Metabolic protections from visceral obesity in aged 2KR mice. (A) ipGTT in male mice at 30-week-old on chow diet feeding. * $p < 0.05$, $n = 12, 12$. (B) Plasma triglycerides during overnight fasting and the following 4-hour refeeding in 31-week-old male mice on chow diet. * $p < 0.05$, $n = 12, 12$. (C-E) 12-13 month old male mice were cold challenged for 6 days and sacrificed at ad libitum. (C) Representative H&E staining of adipose tissues indicating less lipid deposition in BAT and smaller adipocyte in iWAT. Magnifications are at 100x (BAT) and 40x (iWAT). (D-E) qPCR analyses of gene expression in BAT (D) and iWAT (E); * $p < 0.05$, ** $p < 0.01$ for WT vs. 2KR; $n = 5, 7$. (F) 2KR mutant affected different genes from S273A-responsive genes in fat T_{reg} cells isolated from aged mouse eWAT. The detailed gene expression was presented in **Supplemental Table 1**. Data represent means \pm SEM. Student's t -test was used for statistical analyses.



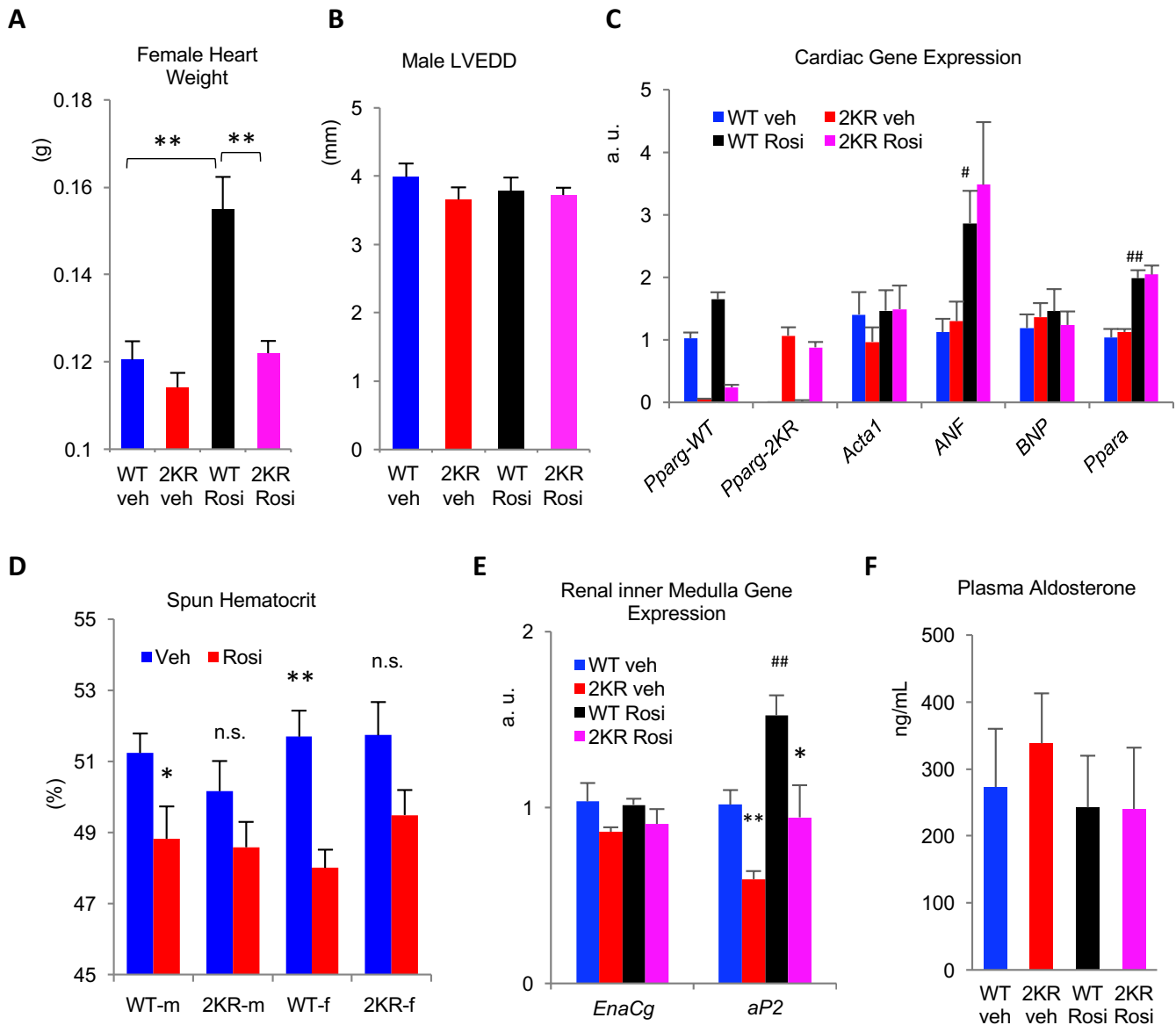
Supplemental Figure 9. Metabolic protections in DIO 2KR mice. (A) Body composition of female mice at 34 weeks of HFD feeding. n=8, 6. (B) Fat depot sizes of female mice on HFD feeding for 34 weeks. Mice were sacrificed after overnight fasting followed by 4-6 hours refeeding. **p<0.01 for WT vs. 2KR; n=8, 6. (C) ipGTT in female mice at 32 weeks on HFD feeding. n=8, 6. (D) Histological analysis of BAT from male mice on prolonged HFD feeding (9 months). Magnifications are at 100x. Mice were sacrificed after fasting overnight. (E) qPCR analyses of gene expression in iWAT of male mice on 24-week HFD feeding. Mice were fasted followed by 4-6 hours refeeding. *p<0.05, **p<0.01 for WT vs. 2KR; n=10, 5. Data represent means \pm SEM. Student's *t*-test was used for statistical analyses.



Supplemental Figure 10. Metabolic responses to rosiglitazone treatment in 2KR mice. (A) Fasting blood glucose levels in female mice after 16 weeks on Rosi treatment. * $p < 0.05$ by Student's *t*-test, $n = 8, 6, 6, 7$. (B) Hepatic cholesterol content in male mice after 24-week Rosi treatment. Mice were sacrificed after overnight fasting. (C) Histological analysis of BAT (at 100x) of male mice after 24-week Rosi treatment by H&E staining. (D-E) Plasma total cholesterol (D) and triglycerides (E) levels during overnight fasting and the following 4-hour refeeding in male mice after 18 weeks on Rosi. In B, D and E, effects of 2KR (* $p < 0.05$, WT versus 2KR) and Rosi (### $p < 0.01$, # $p < 0.05$, veh versus Rosi) by two-way ANOVA ($n = 7, 7, 8, 8$). Data represent means \pm SEM.



Supplemental Figure 11. Improved skeletal remodeling in 2KR mice. (A) DEXA scanning of bone density in male mice after 24-week Rosi treatment, ** $p < 0.01$, $n = 7, 7, 8, 8$. (B) Femur bone density in 7-month-old male mice on chow diet feeding. $n = 12, 12$. (C) Bone density in female mice on 19-week Rosi treatment. ** $p < 0.01$, $n = 8, 6, 6, 7$. (D) Histological analysis of femurs (100x) of male mice on chow, HFD or Rosi treatment by H&E staining. (E) Osmium tetroxide staining of bone marrow adipocytes detected by μ CT scanning in the femurs of male mice after 24-week Rosi treatment. Data represent means \pm SEM. Student's t -test was used for statistical analyses.



Supplemental Figure 12. Cardiac and renal responses to rosiglitazone treatment in 2KR mice. (A) Heart weight in female mice on HFD feeding for 16 weeks and then treated with Rosi for 19 weeks. ** $p < 0.01$, $n = 8, 6, 6, 7$. (B) Left ventricular end-diastolic dimension (LVEDD) in male mice after 24-week Rosi treatment. $n = 7, 7, 7, 8$. (C) Q-PCR measurement of cardiac gene expression in male mice. # $p < 0.05$, ## $p < 0.01$ for WT veh vs. WT Rosi mice; * $p < 0.05$, ** $p < 0.01$ WT vs. 2KR mice under the same treatment, $n = 6, 6, 6, 6$. (D) Spun hematocrit in mice after 15w Rosi treatment. * $p < 0.05$, ** $p < 0.01$; for male mice, $n = 7, 7, 8, 8$; for female mice, $n = 8, 6, 6, 7$. (E) Q-PCR measurement of renal gene expression in male mice. # $p < 0.05$, ## $p < 0.01$ for WT veh vs. WT Rosi mice; * $p < 0.05$, ** $p < 0.01$ WT vs. 2KR mice under the same treatment, $n = 6, 6, 6, 6$. (F) Plasma aldosterone levels in male mice after 24-week Rosi treatment. $n = 7, 7, 7, 8$. Data represent means \pm SEM. Student's t -test was used for statistical analyses.